Available online at www.sciencedirect.com
SCIENCE DIRECT
Sensors and Actuators B 116 (2006) 36–42
SENSORS AND ACTUATORS B CHEMICAL
www.elsevier.com/locate/snb

Concentration normalization with a model of gain control in the olfactory bulb

B. Raman, R. Gutierrez-Osuna *

Department of Computer Science, Texas A&M University, College Station, TX, USA

Received 11 July 2005; received in revised form 17 October 2005; accepted 15 November 2005
Available online 18 April 2006

Abstract

This article presents a biologically inspired model capable of removing concentration effects from the multivariate response of a gas sensor array. The model is based on the first stage of lateral inhibition in the olfactory bulb, which is mediated by periglomerular interneurons. To simulate inputs to the olfactory bulb, signals from a chemosensor array are first processed with a self-organizing model of chemotopic convergence proposed earlier, which leads to odor-specific spatial patterning. Subsequently, a shunting lateral inhibitory network, modeled after the role of periglomerular cells in the olfactory bulb, is used to compress concentration information. The model is validated using experimental data from an array of temperature-modulated metal-oxide chemoresistors.

Keywords: Biologically inspired signal processing; Machine olfaction; Temperature modulation; Self-organized maps; Lateral inhibition

1. Introduction

The input to the olfactory bulb is characterized by massive convergence of olfactory receptor neuron (ORN) axons expressing the same receptor gene onto a single or few target glomeruli [1]. This chemotopic convergence creates compact odor maps that decouple odor quality from intensity. The encoded intensity information at this early stage is transformed by a layer of lateral inhibitory circuits driven by periglomerular interneurons (PG cells). These lateral interactions are known to be of a shunting type (divisive inhibition), and have been hypothesized to serve as a "volume control" mechanism [2], enabling identification of odorants over several log units of concentration. Recently, these glomerular circuits have been found to have center-surround connectivity, and have been suggested to perform pattern normalization, low-band filtration and contrast enhancement [3]. Following these "volume control" circuits, odor signals are further sharpened by another stage of lateral inhibition at the output of the olfactory bulb, mediated by granule cells [4]. The resulting odor signals are then stored in the cortex for subsequent recognition.

Inspired by advances in our understanding of the key processing principles in the olfactory pathway, neuromorphic models for chemical sensor arrays have become a subject of attention in recent years. Ratton et al. [5] employed the olfactory model of Ambros-Ingerson et al. [6], which simulates the closed-loop interactions between the olfactory bulb and higher cortical areas. The model performs a hierarchical processing of an input stimulus into increasingly finer descriptions by repetitive projection of bulbar activity to (and feedback from) the olfactory cortex. Ratton et al. applied the model to classify data from a micro-hotplate metal-oxide sensor excited with a saw-tooth temperature profile. Sensor data was converted into a binary representation by means of thermometer and Gray coding, which was then used to simulate the spatial activity at the olfactory bulb. Their results showed that classical approaches (Gram-Schmidt orthogonalization, fast Fourier transform and Haar wavelets) yield better classification performance. This result should come as no surprise given that the thermometer and Gray codes are unable to faithfully simulate the spatial activity at the olfactory bulb, where the most critical representation of an odor stimulus is formed.

White et al. [7,8] employed a spiking neuron model of the peripheral olfactory system to process signals from fiber-optic sensor array. In their model, the response of each sensor is converted into a pattern of spikes across a population of ORNs,

* Corresponding author. Tel.: +1 979 845 2942; fax: +1 979 847 8578.
E-mail addresses: barani@cs.tamu.edu (B. Raman), rgutier@cs.tamu.edu (R. Gutierrez-Osuna).

0925-4005/$ – see front matter © 2006 Elsevier B.V. All rights reserved.
doi:10.1016/j.snb.2005.11.078

which then projects to a unique mitral cell. Different odors produce unique spatio-temporal activation patterns across mitral cells, which are then discriminated with a delay line neural network (DLNN). Their OB-DLNN model is able to produce a decoupled odor code: odor quality being encoded by the spatial activity across units, and odor intensity by the response latency of the units.

Pearce et al. [9] investigated the issue of concentration hyperacuity by means of massive convergence of ORNs onto GL. Modeling spike trains of individual ORNs as Poisson processes, the authors show that an enhancement in sensitivity by a factor of $\sqrt{n}$ can be achieved at the GL, where n is the number of convergent ORNs. Experimental results on an array of optical micro-beads are presented to validate the theoretical predictions.

Otto et al. employed the KIII model of Freeman et al. [10] to process data from FT-IR spectra [11,12] and chemical sensors [13]. The KIII is a neurodynamics model that faithfully captures the spatio-temporal activity in the olfactory bulb, as observed in electro-encephalogram (EEG) recordings. In [11], the FT-IR spectrum of each analyte was decimated, Hadamard-transformed and normalized before being used as an input vector into the KIII model. The authors showed that the principal components of the mitral cell state-space attractors can be used to discriminate different analytes. Their results, however, indicated that the KIII is unable to match the performance of a regularized discriminant analysis classifier.

Gutierrez-Osuna et al. [14,15] investigated the use of habituation for processing odor mixtures with chemical sensor arrays. A statistical pattern recognition model was presented in [14], where habituation is triggered by a global cortical feedback signal, in a manner akin to Li and Hertz [16]. A neuromorphic approach based on the KIII model was proposed in [15], where habituation is simulated by local synaptic depression of mitral channels. Inspired by the role of GL as functional units [17], sensor array patterns are preprocessed with a family of odor selective discriminant functions before being fed to the KIII model. Their results showed that Hebbian pattern-completion allows the KIII model to recover the majority of the errors, which were introduced in the sensor array and discriminant function stages.

To the best of our knowledge, however, the role of lateral inhibition mediated by PG cells has not been explored for the purpose of processing multivariate signals from chemical sensor arrays. In this paper, we propose a computational model of these gain-control circuits in the olfactory bulb, and analyze its suitability to perform concentration normalization. The model is validated on experimental data from an array of temperature-modulated metal-oxide gas sensors.

2. Proposed model

A fundamental difference between machine and biological olfaction is the dimensionality of the input space. The biological olfactory system employs a large population of ORNs, e.g. 100 million neurons in the human olfactory epithelium, replicated from 1000 primary receptor types [18], whereas its artificial analogue uses very few sensors. In order to narrow this dimensionality gap, we make use of the temperature-selectivity dependence of metal-oxide (MOS) materials [19]. Specifically, we modulate the operating temperature of a MOS sensor with a slow (mHz) sinusoidal waveform, and treat the sensor response at each temperature set point as a "pseudo-sensor," as illustrated in Fig. 1.

To model the chemotopic convergence of ORNs onto glomeruli, we perform a topological clustering of the resulting pseudo-sensors according to their selectivity [20,21]. Formally, we define the selectivity of a pseudo-sensor by its response across a set of Q volatile compounds:

$$\mathrm{ORN}_i = [\mathrm{ORN}_i^{\mathrm{O}_1}, \mathrm{ORN}_i^{\mathrm{O}_2}, \ldots, \mathrm{ORN}_i^{\mathrm{O}_Q}] \quad (1)$$

where $\mathrm{ORN}_i^{\mathrm{O}}$ is the response of ORN_i to odor O, and Q is the number of odorants. We will refer to this Q-dimensional space as the affinity space.

Since GLs are arranged as a single layer in the olfactory bulb, and given that neighboring GL tend to respond to similar odors [22,23], a natural choice to model the ORN-GL convergence is the self-organizing map (SOM) of Kohonen [24]. After training, the distribution of SOM nodes will follow the probability density function of pseudo-sensors in affinity space. Each pseudo-sensor can then be assigned to the closest SOM node (a virtual glomerular unit), thereby forming a convergence map

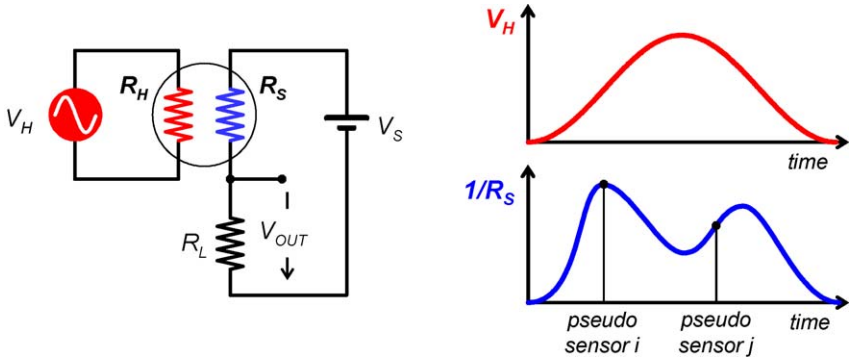

Fig. 1. Temperature modulation for metal-oxide sensors. A sinusoidal voltage V_{H} is applied to a resistive heather R_{H}, and the sensor resistance R_{S} is measured as a voltage drop across a load resistor R_{L} on a half-bridge. Due to the temperature-selectivity dependence, the response of a sensor at a particular temperature can be treated as a separate "pseudo-sensor," and used to simulate a large population of ORNs.

from which the response of each glomerulus can be computed as:

$$G_j^{\mathrm{O}} = \sum_{i=1}^{N} W_{ij} R_i^{\mathrm{O}} \tag{2}$$

where R_i^{O} is the response of pseudo-sensor i to odorant O, N the number of pseudo-sensors, and $W_{ij} = 1$ if pseudo-sensor i converges to SOM node j and zero otherwise. Note that the SOM is used to cluster sensor features that have similar affinities (similar class information), rather than to cluster similar examples as is conventionally done in pattern recognition.

Shunting lateral inhibition by periglomerular interneurons is modeled using a neurodynamics model proposed by Grossberg [25]:

$$\frac{\mathrm{d}x_i^{\mathrm{O}}}{\mathrm{d}t} = -Dx_i^{\mathrm{O}} + (B - x_i^{\mathrm{O}})G_i^{\mathrm{O}} - x_i^{\mathrm{O}} \sum_{k \neq i} c_{ki} G_k^{\mathrm{O}} \tag{3}$$

where G_i^{O} is the activity of SOM node i (i.e., after chemotopic convergence), x_i^{O} the corresponding neuron output to odor O, $-Dx_i^{\mathrm{O}}$ a decay term that models the dynamics of a neuron, $(B - x_i^{\mathrm{O}})G_i^{\mathrm{O}}$ the shunting self-excitation, B the maximum activity of each neuron ($0 \leq x_i^{\mathrm{O}} \leq B$), and $-x_i^{\mathrm{O}} \sum_{k \neq i} c_{ki} G_k^{\mathrm{O}}$ is the shunting inhibition from other neurons [25]. The connection matrix C modeling the shunting inhibition is set as follows:

$$c_{ki} = \begin{cases} U(0,1) & d(k,i) < \dfrac{\sqrt{M}}{r} \\ 0 & \text{otherwise} \end{cases} \tag{4}$$

where $U(a, b)$ is a uniform distribution between a and b, and d is the distance between units measured as an Euclidean distance within the lattice ($d = \sqrt{(\mathrm{row}_k - \mathrm{row}_i)^2 + (\mathrm{col}_k - \mathrm{col}_i)^2}$; row and col being the row and column coordinates of a neuron in the lattice), M the number of SOM nodes, and r determines the width of the lateral inhibitory connections. Self-connections are disabled ($c_{ii} = 0$) to simplify steady-state analysis. Fig. 2 provides an illustration of these three model parameters.

Setting Eq. (3) to zero, it trivially follows that the steady-state output of each neuron is

$$x_i^{\mathrm{O}} = \frac{BG_i^{\mathrm{O}}}{D + G_i^{\mathrm{O}} + \sum_{k \neq i} c_{ki} G_k^{\mathrm{O}}} \tag{5}$$

which, for $c_{ki} = 1 \forall k$, i, and $D = 0$, becomes proportional to the (L1) normalized response of its input relative to the total network activity:

$$x_i^{\mathrm{O}} = \frac{BG_i^{\mathrm{O}}}{\sum_{\forall k} G_k^{\mathrm{O}}} \tag{6}$$

The original study by Grossberg [25] only considered global connections for the purpose of pattern normalization. However, in this work, we show that by adjusting the spread of the lateral inhibitory connections using Eq. (4), the degree of concentration normalization can be controlled parametrically.

3. Results

To validate the model, we have collected a database of temperature-modulated sensor patterns for three analytes: acetone (A), isopropyl alcohol (B) and ammonia (C), at three different concentrations. Three replicas were sampled for each combination of analyte and concentration. Two Figaro MOS sensors (TGS 2600, TGS 2620) [27] were temperature modulated using a sinusoidal heater voltage (0–7 V; 2.5min period; 10 Hz sampling frequency). The response of the two sensors (concatenated) to the three analytes at the three concentration levels (three repetitions each) is shown in Fig. 3. Each point in the temperature cycle was considered as a separate pseudo-sensor, thus resulting in a population of 3000 pseudo-sensors.

The population of pseudo-sensors thus generated is projected onto a GL layer with 400 nodes, arranged as a 20×20 SOM lattice using the convergence model described in Section 2. Only the sensor response to the highest concentration of each analyte was used to generate the SOM convergence map. Fig. 4 shows the odor maps that result from presenting the trained SOM with the sensor response in Fig. 3 (for visualization purposes, only one repetition is shown). It can be clearly seen that the identity of the

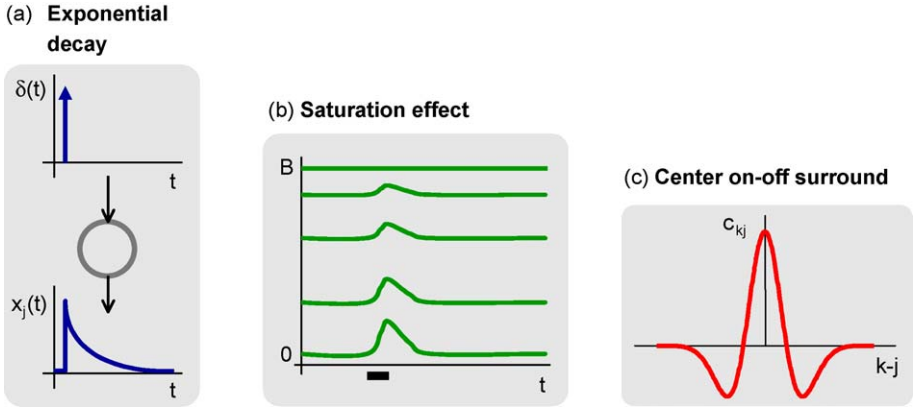

Fig. 2. Illustration of the shunting inhibition model parameters: (a) the term $-Dx_i^{\mathrm{O}}$ in Eq. (3) models the exponential decay; (b) the term $(B - x_i^{\mathrm{O}})G_i^{\mathrm{O}}$ captures saturation effects, according to which the response of a neuron to an input becomes smaller as the neuron's current activation approaches the maximum response level (B) [26]; (c) the connection matrix C which is modeled after a center on–off surround lateral connectivity [3].

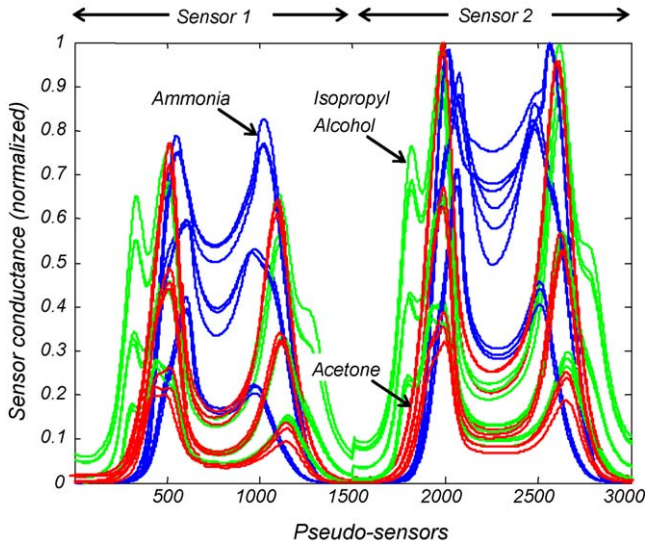

Fig. 3. Temperature-modulated response of two Figaro MOS sensors to three analytes at three concentrations. The top (bottom) three curves for each analyte represent the response of the sensors to the highest (lowest) concentration; three replicates per concentration.

odor is encoded by a unique spatial pattern across SOM nodes, whereas concentration is related to the intensity and spread of this pattern.

The PCA scatterplot of activity across the network is shown in Fig. 5. Without shunting inhibition, the model preserves most of the concentration information. With global inhibition, the network is able to remove most of the concentration information and provide maximum separability between odors. Different degrees of cancellation can be achieved by controlling the spread of the shunting lateral inhibitory connections (for e.g., refer Fig. 5(b)). A detailed characterization of the model is presented in the next section.

4. Characterization of the model

To characterize our model, we employ a measure of separability between categories related to the Fisher's objective function [28]:

$$J = \frac{\text{trace}(S_B)}{\text{trace}(S_W)} \tag{6}$$

where S_W and S_B are the within-class and between-class scatter matrices, respectively, defined as follows:

$$S_W = \sum_{q=1}^{Q} \sum_{x \in \omega_q} (x - \mu_q)(x - \mu_q)^T \tag{7}$$

$$S_B = \sum_{q=1}^{Q} (\mu_q - \mu)(\mu_q - \mu)^T \tag{8}$$

$$\mu_q = \frac{1}{n_q} \sum_{x \in \omega_q} x \quad \text{and} \quad \mu = \frac{1}{n} \sum_{\forall x} x \tag{9}$$

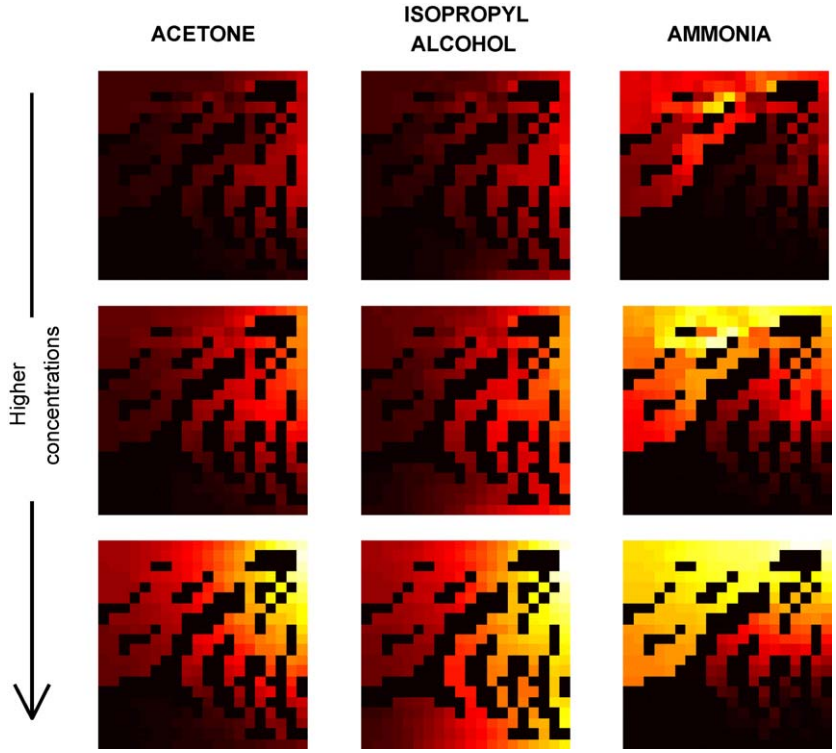

Fig. 4. Spatial odor maps generated by chemotopic convergence of 3000 pseudo-sensors onto a 20 × 20 SOM. Activity of each GL is normalized by the number of ORNs that converge to it.

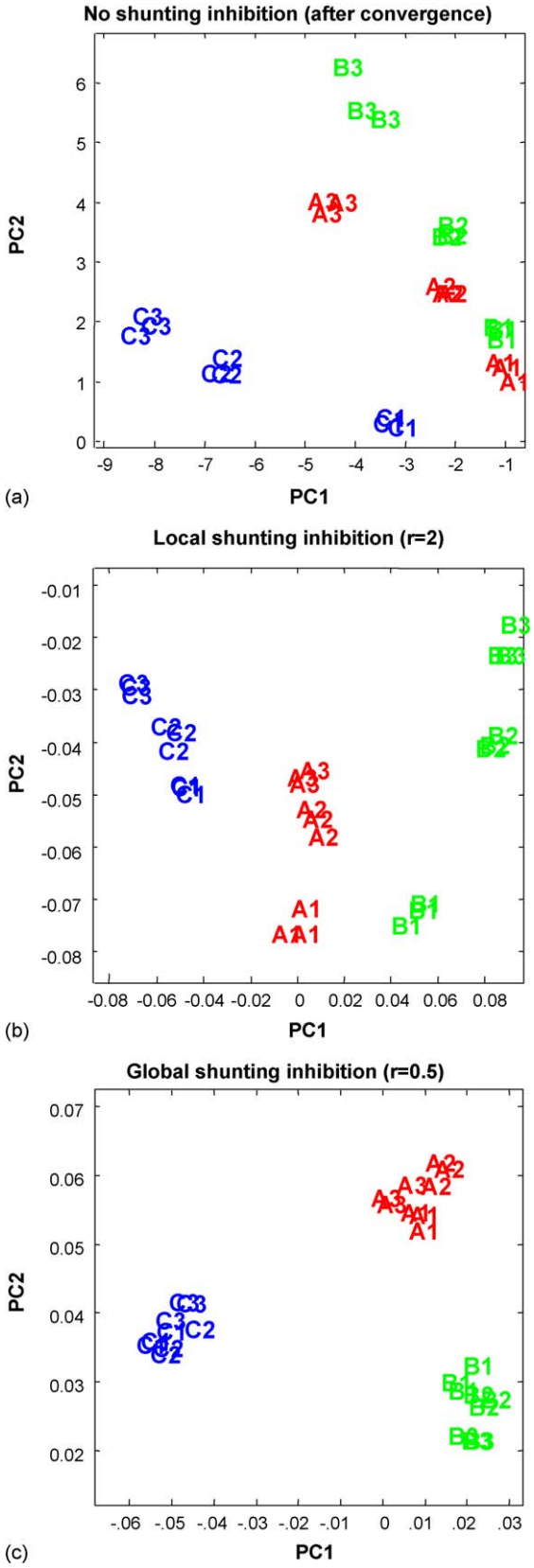

Fig. 5. PCA scatterplot of SOM activity following normalization with the shunting inhibition network (A1: lowest concentration of analyte A, C3: highest concentration of analyte C). Model parameters $B=1$, $D=0.1$. PCA scatterplot of activity across the network (a) after chemotopic convergence (no shunting inhibition), (b) with *local* shunting inhibition, and (c) with *global* shunting inhibition.

where x is the output pattern of the OB model, Q the number of odor classes, μ_q and n_q the mean vector and number of examples for odor q, respectively, n the total number of examples in the dataset, and μ is the mean vector of the entire distribution. Being the ratio of the spread between classes relative to the spread within each class, the measure J increases monotonically as classes become increasingly more separable.

Based on the class separability measure defined in Eq. (6), we define two different measures to quantify the performance of our model: concentration-invariant separability and concentration information. Assuming a three-odor problem, the *concentration-invariant separability* is measured by

$$J_{\text{odor}} = w_1 J_{\text{AB}} + w_2 J_{\text{BC}} + w_3 J_{\text{CA}} \tag{10}$$

where J_{AB}, J_{BC}, and J_{CA} are the separability between odors A and B, B and C, and C and A, respectively, and w_1, w_2, and w_3 are normalization weights to prevent any pair of odors from dominating the metric. The *concentration information* within each odor class is defined by

$$J_{\text{conc}} = w_4 J_{a1a2a3} + w_5 J_{b1b2b3} + w_6 J_{c1c2c3} \tag{11}$$

where J_{a1a2a3}, J_{b1b2b3}, and J_{c1c2c3} are the separability among the three concentrations within an odor, and w_4, w_5, and w_6 are normalization weights to balance the relative contribution of these three terms. In this paper, the normalization weights are determined so that the maximum value of each term ($w_1 J_{\text{AB}}$, $w_2 J_{\text{BC}}$, $w_3 J_{\text{CA}}$, $w_4 J_{a1a2a3}$, $w_5 J_{b1b2b3}$, $w_6 J_{c1c2c3}$) becomes 1 (e.g. $W_1 = 1/\underset{r}{\text{MAX}}(J_{\text{AB}})$).

4.1. Spread of the lateral connections (r)

Fig. 6(a) shows the concentration-invariant separability measure (J_{odor}) as a function of the width of the shunting inhibitory connections. Maximum separability between odors is achieved for small r (global connections). As illustrated in the scatterplot of Fig. 5(c), global connections remove most of the concentration information, a result that also follows from the steady-state response in Eq. (5). In contrast, reduction in the width of the shunting inhibition allows the within-class scatter to increase, which is mostly due to concentration effects, thereby reducing J_{odor}.

Fig. 6(b) shows the *concentration information* measure (J_{conc}) as a function of the width of the shunting inhibitory connections. Maximum separability is achieved for no shunting inhibition ($r=20$, for our 20×20 SOM). In this case concentration information serves as the principal source of variance, as shown in Fig. 5(a). As the connections become global, most of the concentration information is removed. Between these two extremes (global inhibition versus none), different degrees of separability can be achieved among concentration levels of the same odor.

The width of the lateral inhibition can therefore be used to provide an appropriate tradeoff between odor class information (between-class scatter) and odor concentration information (within-class scatter).

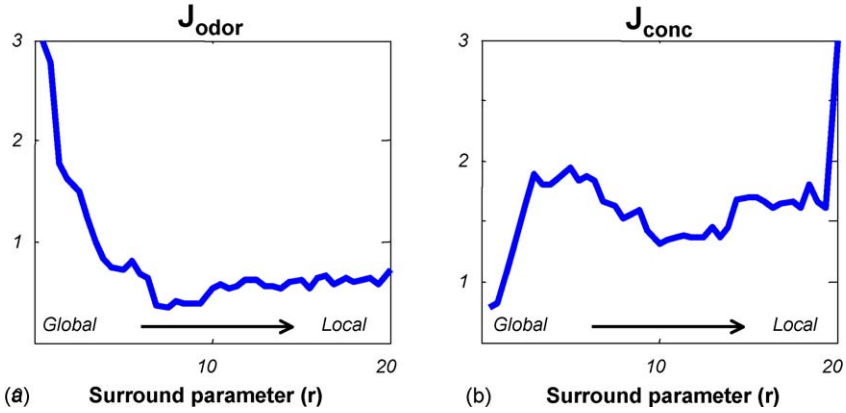

Fig. 6. Characterization of the model; small r represents global connections, and large r represents local connections. (a) Measure of concentration-invariant separability (J_{odor}) as a function of the width of shunting lateral inhibition. (b) Measure of concentration information (J_{conc}) as a function of the width of shunting lateral inhibition.

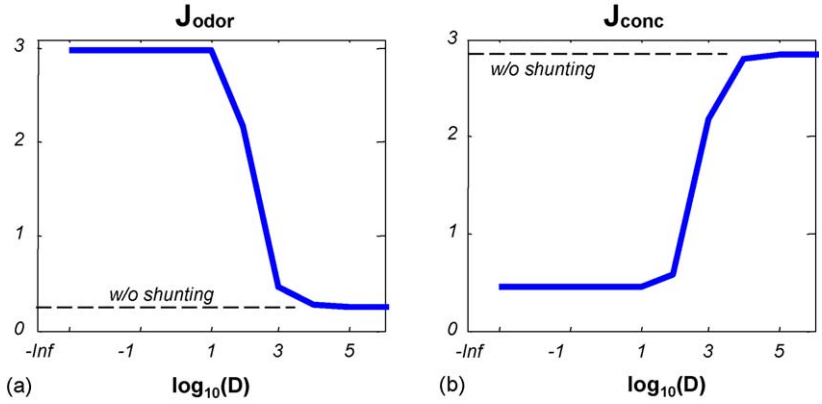

Fig. 7. Characterization of the exponential decay rate (D). (a) Concentration-invariant separability (J_{odor}) as a function of the decay parameter D. (b) Concentration information (J_{conc}) as a function of the decay parameter D (model parameters $r = 0.5$ and $c_{ki} = 1 \forall k, i$). Dashed line indicates separability without shunting inhibition.

4.2. Rate of exponential decay (D)

Fig. 7(a and b) shows the *concentration-invariant separability* and *concentration information* measures as a function of decay rate D. For small value of D ($D \ll \sum_k G_k^O$), the model achieves concentration compression similar to the L1 norm, thereby improving separability between odors, as shown in Fig. 7(a). For large D values ($D \gg \sum_k G_k^O$), the steady-state response of the model is a scaled version of its inputs and hence the model retains all the concentration information, as shown in Fig. 7(b). Therefore, for a fixed spread of lateral connections, the exponential decay rate D can also be used to control the amount of concentration compression.

5. Conclusion

We have presented a neurodynamic model of the first stage of lateral inhibition in the olfactory bulb, which is mediated by periglomerular interneurons. Our results show that global connections remove most of the concentration information, increasing the separability between odors. Local connections, on the other hand, retain most of the concentration information at the expense of discriminatory power among odor classes. Thus, different degrees of concentration normalization can be achieved by modulating the width of the lateral connections (or the rate of decay of the neurons). Our study has analyzed the role of periglomerular inhibition in isolation. The next stage of this work is the integration of this gain-control model with models of contrast enhancement at the output of the olfactory bulb [21], and feedback from cortical circuits [30].

Christensen et al. have recently suggested that local neurons (analogous to PG cells) in the antennal lobe (analogous to the mammalian olfactory bulb) of sphinx moth can operate as multifunctional units, causing local inhibition at lower odor concentrations and global inhibition at higher concentrations [29]. Their study is particularly relevant to our work because it identifies a possible biological mechanism for modulating inhibitory width. The results presented in our article (particularly those in Section 4.1) can therefore be used to predict the effect that modulation of inhibitory width may have during the processing of odor signals.

Acknowledgments

This material is based upon work supported by the National Science Foundation under CAREER award 9984426/0229598.

Takao Yamanaka, Agustin Gutierrez-Galvez and Alexandre Perera-Lluna are gratefully acknowledged for valuable suggestions during the preparation of this manuscript.

References

[1] R. Vassar, S.K. Chao, R. Sitcheran, J.M. Nunez, L.B. Vosshall, R. Axel, Topographic organization of sensory projections to the olfactory bulb, Cell 79 (1994) 981–991.
[2] W. Freeman, Olfactory system: odorant detection and classification, in: D. Amit, G. Parisi (Eds.), Building Blocks for Intelligent Systems: Brain Components as Elements of Intelligent Function. Part 2, vol. III, Academic Press, New York, 1999.
[3] J.L. Aungst, P.M. Heyward, A.C. Puche, S.V. Karnup, A. Hayar, G. Szabo, M.T. Shipley, Center-surround inhibition among olfactory bulb glomeruli, Nature 26 (2003) 623–629.
[4] K. Mori, H. Nagao, Y. Yoshihara, The olfactory bulb: coding and processing of odor molecule information, Science 286 (1999) 711–715.
[5] L. Ratton, T. Kunt, T. McAvoy, T. Fuja, R. Cavicchi, S. Semancik, A comparative study of signal processing techniques for clustering microsensor data (a first step towards an artificial nose), Sens. Actuators B: Chem. 41 (1997) 105–120.
[6] J. Ambros-Ingerson, R. Granger, G. Lynch, Simulation of paleocortex performs hierarchical clustering, Science 247 (1990) 1344–1348.
[7] J. White, T.A. Dickinson, D.R. Walt, J.S. Kauer, An olfactory neural network for vapor recognition in an artificial nose, Biol. Cybern. 78 (1998) 245–251.
[8] J. White, J.S. Kauer, Odor recognition in an artificial nose by spatiotemporal processing using an olfactory neuronal network, Neurocomputing 26–27 (1999) 919–924.
[9] T.C. Pearce, P.F.M.J. Verschure, J. White, J.S. Kauer, Robust stimulus encoding in olfactory processing: hyperacuity and efficient signal transmission, in: S. Wermter, J. Austin, D. Willshaw (Eds.), Emergent Neural Computation Architectures Based on Neuroscience, Springer-Verlag, 2001, pp. 461–479.
[10] H.J. Chang, W.J. Freeman, B.C. Burke, Biologically modeled noise stabilizing neurodynamics for pattern recognition, Int. J. Bifurcat. Chaos 8 (1998) 321–345.
[11] S. Quarder, U. Claussnitzer, M. Otto, Using singular-value decompositions to classify spatial patterns generated by a nonlinear dynamic model of the olfactory system, Chemometr. Intell. Lab. Syst. 1248 (2001) 45–51.
[12] U. Claussnitzer, S. Quarder, M. Otto, Interpretation of analytical patterns from the output of chaotic dynamical memories, Fresen. J. Anal. Chem. 369 (2001) 698–703.
[13] M. Otto, S. Quarder, U. Claußnitzer, J. Lerchner, A nonlinear dynamic system for recognizing chemicals based on chemical sensors and optical spectra, in: Proceedings of the World Multiconference on systemics, Cybernetics and Informatics (SCI-2000), vol. X, 2000, pp. 413–418.
[14] R. Gutierrez-Osuna, N.U. Powar, Odor mixtures chemosensory adaptation in gas sensor arrays, Int. J. Artif. Intell. Tools 12 (2003) 1–16.
[15] R. Gutierrez-Osuna, A. Gutierrez-Galvez, Habituation in the KIII olfactory model with chemical sensor arrays, IEEE Trans. Neural Networks 16 (2003) 649–656.
[16] Z. Li, J. Hertz, Odor recognition and segmentation by a model olfactory bulb and cortex, Network: Comput. Neural Syst. 11 (2000) 83–102.
[17] T.C. Pearce, Computational parallels between the biological olfactory pathway and its analogue 'The electronic nose'. Part I. Biological olfaction, BioSystems 41 (1997) 43–67.
[18] L. Buck, R. Axel, A novel multigene family may encode odorant receptors: a molecular basis for odor recognition, Cell 85 (1991) 175–187.
[19] A.P. Lee, B.J. Reedy, Temperature modulation in semiconductor gas sensing, Sens. Actuators B: Chem. 60 (1990) 35–42.
[20] R. Gutierrez-Osuna, A Self-organizing model of chemotopic convergence for olfactory coding, in: Proceedings of the 2nd Joint EMBS-BMES Conference, Houston, TX, 2002, pp. 23–26.
[21] B. Raman, R. Gutierrez-Osuna, A. Gutierrez-Galvez, A. Perera-Lluna, Sensor-based machine olfaction with a neurodynamics model of the olfactory bulb, in: Proceedings of the 2004 IEEE/RSJ International Conference on Intelligent Robots and Systems, Sendai, Japan,: Chem September–2 October, 2004.
[22] M. Meister, T. Bonhoeffer, Tuning and topography in an odor map on the rat olfactory bulb, J. Neurosci. 21 (2001) 1351–1360.
[23] B.A. Johnson, M. Leon, Modular representation of odorants in the glomerular layer of the rat olfactory bulb and the effects of stimulus concentration, J. Compar. Neurol. 422 (2000) 496–509.
[24] T. Kohonen, Self-organized formation of topologically correct feature maps, Biol. Cybern. 43 (1982) 59–69.
[25] S. Grossberg, Adaptive pattern classification and universal recording. Part I. Parallel development and coding of neural feature detectors, Biol. Cybern. 23 (1976) 121–134.
[26] W. Gerstner, W. Kistler, Spiking Neuron Models: Single Neurons, Populations, Plasticity, University Press, Cambridge, 2002.
[27] Figaro 1996, Figaro Engineering Inc., Osaka, Japan.
[28] K. Fukunaga, Introduction to Statistical Pattern Recognition, 2nd ed., Academic Press, New York, 1990.
[29] T.A. Christensen, G. D'Alessandro, J. Lega, J.G. Hildebrand, Morphometric modeling of olfactory circuits in the insect antennal lobe. Part I. Simulations of spiking local interneurons, Biosystems 61 (2001) 143–153.
[30] B. Raman, R. Gutierrez-Osuna, Mixture segmentation and background suppression in chemosensor arrays with a model of olfactory bulb-cortex interaction, accepted for publication in 2005, in: IEEE International Joint Conference on Neural Networks, Montreal, Canada, 31 July–4 August, 2005.

Biographies

Baranidharan Raman received his Bachelor of Engineering in Computer Science with distinction from the University of Madras in 2000, and the M.S. degree in Computer Science from Texas A&M University in 2003. He is currently a Ph.D. candidate in the Department of Computer Science, Texas A&M University. His research interests include sensor based machine olfaction, machine learning, neural computation, bio-mimetic systems, interfaces for human-computer interaction, face recognition and robotics.

Ricardo Gutierrez-Osuna received the B.S. degree in Electrical Engineering from the Polytechnic University of Madrid in 1992, and the M.S. and Ph.D. degrees in Computer Engineering from North Carolina State University in 1995 and 1998, respectively. From 1998 to 2002 he served on the faculty at Wright State University. He is currently an assistant professor of Computer Engineering at Texas A&M University. His research interests include pattern recognition, neuromorphic computation, machine olfaction, and speech-driven facial animation.